Kinetic Analysis of Controlled/"Living" Radical Polymerizations by Simulations. 1. The Importance of Diffusion-Controlled Reactions

Devon A. Shipp and Krzysztof Matyjaszewski*

Department of Chemistry, Carnegie Mellon University, 4400 Fifth Avenue, Pittsburgh, Pennsylvania 15213

Received December 11, 1998; Revised Manuscript Received March 3, 1999

ABSTRACT: Controlled/"living" atom transfer radical polymerization (ATRP), which is subject to the persistent radical effect, has been examined through computer simulations. It was found that the peculiar time-dependent rates predicted by the persistent radical effect may not be observed experimentally because termination is dependent on chain length and viscosity. In the early stages of the polymerizations the deactivating species is produced very fast through irreversible radical−radical termination; however, as the polymerization progresses, less deactivator is produced because termination reactions are slowed, thus resulting in a steady rate of polymerization. Thermal initiation of styrene was found to be insignificant in ATRP under the conditions examined, in contrast to systems characterized by a low equilibrium constant, such as TEMPO-mediated polymerization, where the rate of styrene polymerization is dominated by thermal initiation. Inclusion of termination rate coefficients that decrease during polymerization in the simulation model led to adequate reproduction of experimental results.

Introduction

The field of controlled/"living" radical polymerization has flourished in recent years.[1] In particular, both stable free radical polymerization[1−9] and atom transfer radical polymerization (ATRP)[10−17] have generated great interest in industry and academia. A very recent addition to this field is the variation of the degenerative transfer technique[18,19] called reversible addition−fragmentation chain transfer (RAFT) polymerization.[20] All these techniques allow the synthesis of polymers that may have predetermined molecular weights, narrow molecular weight distributions, and novel architecture.[21,22] Perhaps the most significant advantage of these methods over conventional radical polymerization, however, is that polymers potentially have functionality that allows further chemistry to be performed on the polymer, such as cross-linking reactions, exchange of functional groups, and block copolymerization.[1]

Through such interest, the mechanisms and kinetics of these controlled polymerizations have also been examined in some detail. However, both of these very important facets of the polymerizations remain poorly understood. Substantial progress was made in understanding when it was realized[7,23,24] that stable free radical polymerization and ATRP are subject to the *persistent radical effect*,[25] a concept proposed by Fischer[26] to explain the selectivities observed in a variety of radical reactions. Subsequent work by Fischer[23] has indicated that persistent radical effect predicts peculiar time dependencies for monomer consumption, persistent radical evolution, and growing (transient) radical concentration. Johnson et al.[24] previously produced similar qualitative observations during an examination of the kinetics of the stable free radical polymerization of acrylates using simulations. In a recent paper, Kothe et al.[27] have provided convincing evidence through model studies that the persistent radical effect does indeed operate in the decomposition of alkoxyamines, the "initiator" within stable free radical polymerization.

However, these odd dependencies have generally not been observed in controlled polymerization experiments, at least not to the extent predicted by the persistent radical effect. This has prompted us to examine why this may be the case. There may be several causes for this discrepancy, including poor experimental data, the persistent radical effect as discussed is not fully valid, or other phenomena such as inhomogeneity, aggregation, and/or deactivation of the catalyst. However, perhaps the simplest explanation lies in the fact that ATRP is generally taken to quite high monomer conversion, and therefore the viscosity of the medium increases dramatically. This, in turn, may affect the rates of several reactions involved in the polymerization. Therefore, in this paper we explore how diffusion-controlled rate coefficients affect the kinetics of controlled/"living" ATRP.

Scheme 1

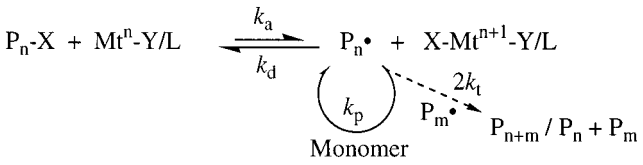

Results and Discussion

Model Development. In general terms, the basis of ATRP is a metal (Mt^n/L, where L = ligand) catalyzed dynamic equilibrium (Scheme 1) between dormant (P−X) and active species (P•), where the latter are free radicals capable of propagating.[21] This process also generates a "counter radical" (X−Mt^{n+1}/L) that is persistent and reacts (almost) selectively with the active species and not with itself. The equilibrium as indicated in Scheme 1 lies heavily in favor of the dormant species, such that the concentration of radicals is low relative to the combined concentrations of dormant and active chains.

Another requirement for controlled/"living" polymerization is that initiation is fast relative to propagation; all chains should be initiated approximately at the same time.[28] For a radical polymerization without the activa-

10.1021/ma9819135 CCC: $18.00
Published on Web 04/09/1999

tion/deactivation cycle, this would result in a large amount of termination occurring and therefore loss of the active centers. The equilibrium established between the dormant and active species during ATRP allows initiation of all chains to occur quickly but with a low radical concentration present.

However, the finite concentration of free radicals means that radical−radical termination is never fully suppressed. Furthermore, with each termination reaction between two free radicals, there is also 2 equiv of deactivator generated. Because the deactivator is persistent and builds in concentration during the polymerization, the equilibrium is shifted toward the dormant species, thus slowing the reaction down. This is the basis of the persistent radical effect, and Fischer[23] has shown that it should result in nonlinear first-order kinetics with respect to monomer consumption. Fischer's analysis divided the reaction time into three segments:[23,27] (1) very short times ($<10^{-3}$ s), (2) intermediate times ($\sim 10^{-3}$ s $< t < 5 \times 10^2$ h), and (3) very long times ($>3 \times 10^3$ years). Of practical interest is the intermediate regime only, where it was shown the monomer consumption should follow eq 1.[23] The concentrations of the active species (radicals) and persistent species (Mt^{n+1} in ATRP) are described by eqs 2 and 3 respectively.[23,27]

$$\ln\left(\frac{[M]_0}{[M]}\right) = \frac{3}{2}k_p([RX]_0[Mt^n]_0)^{1/3}\left(\frac{k_a}{3k_d 2k_t}\right)^{1/3} t^{2/3} \quad (1)$$

$$[P^\bullet] = ([RX]_0[Mt^n]_0)^{1/3}\left(\frac{k_a}{3k_d 2k_t}\right)^{1/3} t^{-1/3} \quad (2)$$

$$[Mt^{n+1}] = ([RX]_0[Mt^n]_0)^{2/3}\left(\frac{3k_a{}^2 2k_t}{k_d{}^2}\right)^{1/3} t^{1/3} \quad (3)$$

To examine the kinetics of polymerizations subject to the persistent radical effect, computer simulations are extremely useful because one can omit or modify reactions and then note the effects to apparent rates of reactions. However, such a procedure is completely reliant upon both an accurate model and accurate data and often limited because it is computer time and memory intensive. This last point has been overcome (at least partially) by the implementation of the Predici program package[29] that allows simulations of polymerizations up to very high degrees of polymerizations without losing too much information through simplifications in the model. Several previous studies[7,29−33] have shown that the package is versatile enough to allow the incorporation of many reactions. Therefore, we have used this program for our analysis of controlled/"living" polymerizations.

Scheme 2 outlines the general model for these polymerizations. Included are the following reactions and associated rate constants/coefficients: (a) activation and deactivation of the initiator (RX; k_a, k_d), (b) addition of monomer to the initiating radical (R•; k_i), (c) thermal initiation (k_{therm}), (d) activation and deactivation of polymeric dormant species (P_nX; k_a, k_d), (e) propagation (k_p), (f) termination of two initiating radicals (k_{t0}), (g) macromolecular radical−radical termination by both combination and disproportionation (k_{tc}, k_{td}), (h) primary radical termination (k_{tP}), and (i) transfer to monomer ($k_{tr,M}$). Other reactions, such as transfer to polymer and chain end degradation,[34] have been neglected, as they are insignificant in the systems studied here. Table 1 contains the data used in the simulations, with the parameters that are adjusted (e.g., termination rate coefficients and concentrations) indicated. The contribution of styrene thermal initiation will be discussed further below. A third-order model is used, with a rate constant (k_{therm}) taken from Hui and Hamielec,[35] but it must be kept in mind that the rate constant from this work was obtained with a specific polymerization model, which included a conversion-dependent (i.e., viscosity and chain length dependent) k_t. Therefore, using this

Scheme 2

Initiation

$$R\text{-}X + Mt^n\text{-}Y/L \underset{k_d}{\overset{k_a}{\rightleftharpoons}} R^\bullet + X\text{-}Mt^{n+1}\text{-}Y/L$$

$$R^\bullet + M \xrightarrow{k_i} P_1^\bullet$$

$$3\ M \xrightarrow{k_{therm}} 2\ R^\bullet$$

Propagation

$$P_n\text{-}X + Mt^n\text{-}Y/L \underset{k_d}{\overset{k_a}{\rightleftharpoons}} P_n^\bullet + X\text{-}Mt^{n+1}\text{-}Y/L$$

$$P_n^\bullet + M \xrightarrow{k_p} P_{n+1}^\bullet$$

Termination

$$2\ R^\bullet \xrightarrow{k_{t0}} D_2$$

$$P_n^\bullet + P_m^\bullet \xrightarrow{k_{tc}} D_{n+m}$$

$$P_n^\bullet + P_m^\bullet \xrightarrow{k_{td}} D_n + D_m$$

$$P_n^\bullet + R^\bullet \xrightarrow{k_{tP}} D_n$$

Chain Transfer

$$P_n^\bullet + M \xrightarrow{k_{tr,M}} D_n + R^\bullet$$

Table 1. Standard Parameters Used in ATRP Simulations

parameter	value	ref
k_i (L mol^{-1} s^{-1})	16000	41, 42
k_p (L mol^{-1} s^{-1})	1600	67
$2k_{tc}(0)$ (L mol^{-1} s^{-1})[a]	1×10^9	41
$2k_{td}(0)$ (L mol^{-1} s^{-1})[a]	1×10^8	41
$2k_{t0}$ (L mol^{-1} s^{-1})	5×10^9	41
$k_{tr,M}$ (L mol^{-1} s^{-1})	0.22	68
k_d (L mol^{-1} s^{-1})[a]	1.1×10^7	63
k_a (L mol^{-1} s^{-1})	0.45	63
k_{tP} (L mol^{-1} s^{-1})	1×10^9	41, 43
k_{therm} (L mol^{-1} s^{-1})[a]	4.8×10^{-11}	35
$[M]_0$ (M)[a]	8.7	
$[RX]_0$ (M)[a]	0.087	
$[Mt^n]_0$ (M)[a]	0.087	
$[Mt^n+1]_0$ (M)	0	
temperature (°C)	110	

[a] Parameter varied in some simulations. See text and figure captions.

rate constant in the context of another model that also incorporates a conversion-dependent k_t will actually overestimate the rate of thermal polymerization. However, for illustrative purposes only, the Hui and Hamielec data will be adequate.

Chain Length- and Diffusion-Dependent Rate Constants. The diffusion-controlled dependence of the termination rate constant has been known for some time.[36−38] However, there is evidence that suggests that rate constants of other processes involved in free radical polymerization are also dependent either on chain length, conversion of monomer to polymer (viscosity), or both. Propagation becomes diffusion-controlled when the polymerization medium becomes very viscous, such as at very high conversions. There is also evidence that suggests that the first few propagation steps occur at a much faster rate than the overall propagation rate.[39−42] This difference is due to a decrease in the translational and rotational degrees of freedom that occurs as the chain grows.[40] Within the model for the controlled/"living" systems proposed here, the activation and deactivation rates are also potentially chain length dependent. Given this background, it is worthwhile examining these possibilities.

While the termination rate is known to be diffusion-controlled, this fact is often neglected in order to simplify the kinetic analysis of polymerization. This was also the case in the Fischer's analysis of the persistent radical effect in controlled/"living" stable free radical polymerization[23] and also in the work of Johnson et al.[24] There are many studies that indicate that the termination rate coefficient (rather than a constant) can change by several orders of magnitude during the course of a polymerization.[38] In solution (i.e., at low viscosities), the termination rate coefficient for small organic radicals is of the order of 10^9 M^{-1} s^{-1}.[41,43] Measurements of polymeric radical termination result in rate coefficients from 10^8 M^{-1} s^{-1} to less than 10^5 M^{-1} s^{-1} for low to high conversions, respectively.[38,44,45]

The problem with attempting to model a diffusion-controlled termination rate coefficient is the choice of a model or, in other words, an analytical expression for how k_t changes as a function of conversion. Some workers, such as Benson and North,[37] Allen and Patrick,[36] and others,[46−52] have used the Smoluchowski model to describe these processes as a function of chain length at low polymer concentrations. Others have used a simple power law,[53−58] or more complex expressions,[44] to describe k_t as a function of chain length at both low and high monomer conversions.

Such changes in k_t will be determined by several parameters, including molecular weight, the T_g of the system, temperature, and polymer concentration. However, Gilbert and co-workers[59,60] have very recently found that normalized diffusion coefficients of oligomeric methacrylates and styrenes in polymer solutions vary according to a simple, empirical relationship given in eq 4

$$D_{DP}/D_1 = DP^{-(0.664+2.02w_p)} \tag{4}$$

where DP is the degree of polymerization and w_p is the weight fraction of polymer. Surprisingly, this relationship seemed invariant of temperature (studied between 25 and 50 °C), oligomer type (methacrylates or styrene), and polymer matrix type (poly(methyl methacrylate), poly(butyl methacrylate), polystyrene), and extrapolation from monomer and dimer diffusion data adequately predicted the diffusion behavior of higher oligomers (DPs < 10 were examined). While some simulation conditions fall outside the bounds of the diffusion measurements of Gilbert et al.,[59] the apparent "universality" and simplicity of eq 4 are very appealing, and therefore an equation of this type was used in our simulations to impart a conversion/chain length dependence on k_t. There are two caveats worth noting at this stage. First, it was found that using other models for the reduction of k_t led to similar results as those that used eq 4 (i.e., the qualitative observations presented here are model-independent). Second, we realize that eq 4 probably does not represent a physically correct description of how k_t changes in these polymerizations; however, it does allow us to qualitatively alter k_t throughout the reaction in a simple fashion.

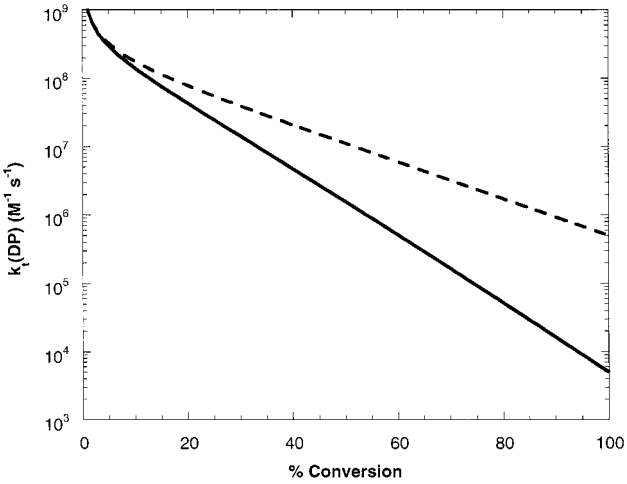

Figure 1. Change in k_t(DP) as a function of conversion in bulk, $k_t(DP) = 10^9 DP^{-(0.65+0.02DP)}$ (—), and in 50% solution polymerization, $k_t(DP) = 10^9 DP^{-(0.65+0.01DP)}$ (- - -).

The conditions of controlled/"living" polymerization provide a special case for the termination step. In these experiments, the chain lengths of both radicals can be approximated as being the same. This is in contrast to conventional free radical polymerization where it is thought that termination is dominated by the reaction between short−short and short−long chains.[46,47] With this approximation, one can simplify some of the chain-length-dependent expressions (such as the Smoluchowski equation) into a more simple scaling law. Furthermore, the simulations presented here aim for a degree of polymerization at 100% monomer conversion of 100. Therefore, in the ideal situation, the percentage conversion equals chain length. A simple scaling law of the form of eq 5 which is based upon the equation of Gilbert et al.[59] was used,

$$k_t(DP) = k_t(0)DP^{-(0.65+0.02DP)} \tag{5}$$

where DP is calculated from conversion of monomer to polymer ($DP = \Delta[M]/[RX]_0$) and considering the initiator being the first unit (DP = 1−101). Figure 1 shows how k_t(DP) varies as a function of conversion for two cases: for bulk polymerization and for a 50% solution polymerization. The difference between these two cases arises from the fact that at 100% conversion the solution polymerization will only have 50% polymer in solution and therefore a lower viscosity. In terms of eq 5, this meant the 0.02 term in the exponent is halved for the

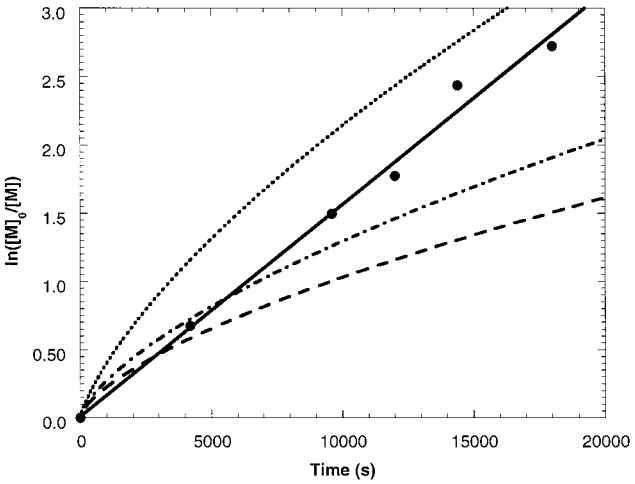

Figure 2. First-order kinetic plot of monomer consumption in the ATRP of styrene for experiment (●, with straight line fit, —)[62] and simulations (lines) with parameters given in Table 1; $k_{therm} = 0$ and constant k_t (– – –, $k_{tc} = 10^8$, $k_{td} = 10^7$), (- · -, $k_{tc} = 5 \times 10^7$, $k_{td} = 5 \times 10^6$), (···, $k_{tc} = 10^7$, $k_{td} = 10^6$).

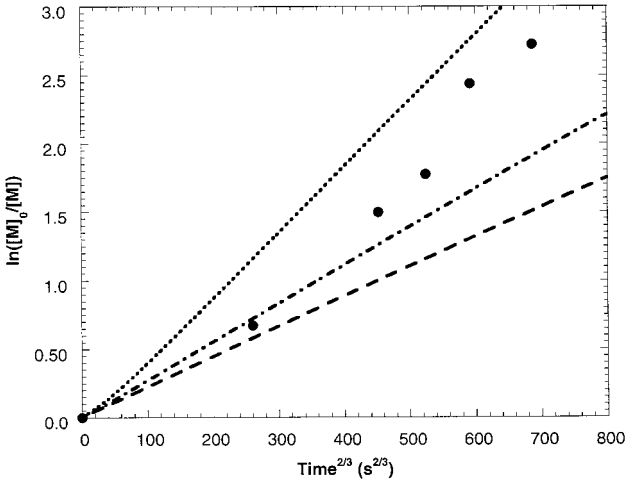

Figure 3. First-order kinetic plot of monomer consumption, as a function of time$^{2/3}$, in the ATRP of styrene for experiment (●)[62] and simulations (lines; as in Figure 2) with parameters given in Table 1; $k_{therm} = 0$ and constant k_t (– – –, $k_{tc} = 10^8$, $k_{td} = 10^7$), (- · -, $k_{tc} = 5 \times 10^7$, $k_{td} = 5 \times 10^6$), (···, $k_{tc} = 10^7$, $k_{td} = 10^6$).

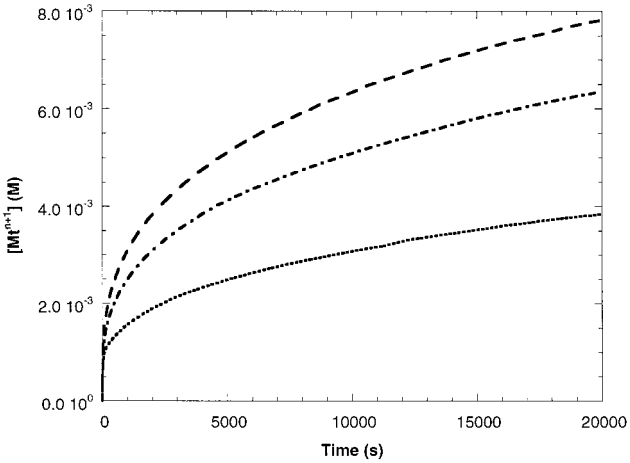

Figure 4. [Mt^{n+1}] as a function of time in the ATRP of styrene for simulations (as in Figure 2) with parameters given in Table 1; $k_{therm} = 0$ and constant k_t (– – –, $k_{tc} = 10^8$, $k_{td} = 10^7$), (- · -, $k_{tc} = 5 \times 10^7$, $k_{td} = 5 \times 10^6$), (···, $k_{tc} = 10^7$, $k_{td} = 10^6$).

solution polymerization simulations. Equation 5 was used to alter both the combination and disproportionation rate coefficients, whose initial magnitudes were chosen to reflect >90% combination in styrene polymerization.[61]

At very high conversions the propagation step may become diffusion-controlled.[61] However, this may only occur in the final stages of the polymerization and thus is neglected in our simulations. The addition of small (monomeric) radicals to monomer (i.e., initiation) has been studied extensively[41,42] and often occurs at a rate that is at least an order of magnitude faster than the rate of monomer addition to polymeric radicals. There is also some evidence that suggests that the first few propagation steps may be faster than the overall propagation rate,[39,41] and the first propagation step may be approximately an order of magnitude faster than the subsequent additions.[39,40] Often in ATRP, the radicals formed from the initiator are models for the propagating radicals. In our model, therefore, we have chosen the rate constant for initiation to be an order of magnitude greater than the propagation rate constant.

The extent of diffusion control of the activation and deactivation reactions in controlled/"living" polymerizations has not been examined. It is possible that the activation reaction is chemically controlled throughout most of the polymerization, whereas the deactivation reaction may be diffusion-controlled if the viscosity is sufficiently high. To keep the model as simple as possible, we have used constant rates of activation and deactivation for both the initiator and polymeric chains; however, we also examine what effect changing the rate constant of deactivation has on polymerization rates.

Idealized Persistent Radical Effect in ATRP: No Diffusion-Dependent Termination. It is worthwhile to begin with simulations that exclude any diffusion-controlled termination, thus confirming the existence of the persistent radical effect in these systems. Figure 2 shows the first-order kinetic plot of styrene consumption in ATRP simulations, along with data taken from experiments of this system.[62] The experimental data give a linear dependence, which is an indication of a constant number of growing radicals present in the system and is contrary to the prediction of the persistent radical effect.[23] The simulations, on the other hand, with a constant value for the termination rate coefficient, show a marked curvature throughout the polymerization.

Figure 3 contains the data from Figure 2, but plotted as a function of $t^{2/3}$, as suggested by eq 1. Here the experimental data points do not lie on a straight line; however, the simulated data are linear. From this it appears that the ATRP simulations are consistent with the persistent radical effect and eqs 1−3; however, the experimental styrene ATRP system is not. Further evidence of this can be seen in Figures 4 and 5, where the deactivator concentrations ([Mt^{n+1}]) are plotted against t and $t^{1/3}$, respectively. Figure 4 shows that Mt^{n+1} is continuously generated during the polymerizations as a result of radical−radical termination. The amount of Mt^{n+1} depends on the value of the rate coefficient for termination; the higher the value, the more Mt^{n+1} is generated, and thus the slower the polymerization (see Figure 2). Fischer's kinetic analysis[23] of the persistent radical effect predicts that the deactivator (or persistent species) should increase in concentration as a function of $t^{1/3}$ (eq 3). Figure 5 bears this out; for each simulation, [Mt^{n+1}] increases in a

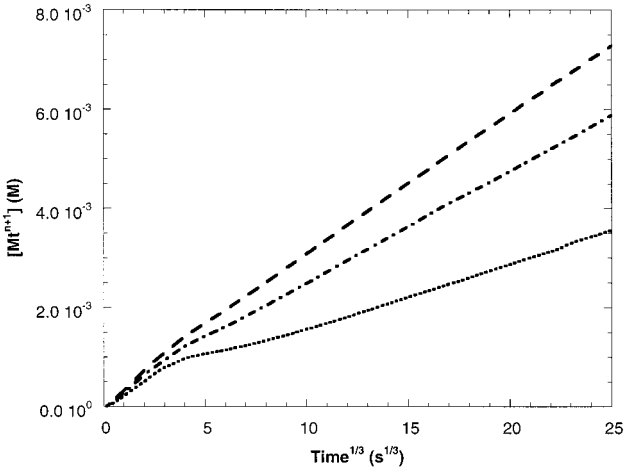

Figure 5. $[Mt^{n+1}]$ as a function of time$^{1/3}$ in the ATRP of styrene for simulations (as in Figure 2) with parameters given in Table 1; $k_{therm} = 0$ and constant k_t (– – –, $k_{tc} = 10^8$, $k_{td} = 10^7$), (-·-, $k_{tc} = 5 \times 10^7$, $k_{td} = 5 \times 10^6$), (···, $k_{tc} = 10^7$, $k_{td} = 10^6$).

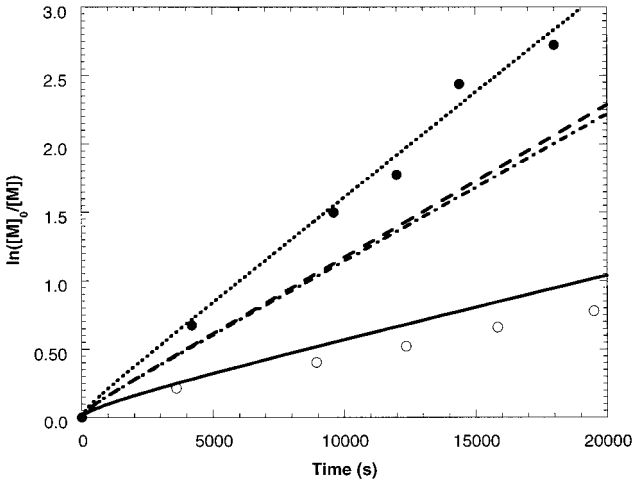

Figure 6. Dependence of the first-order kinetic plot of monomer consumption in the ATRP of styrene on conversion-dependent k_t, k_d, and k_{therm}. Experiment (●, bulk; ○, 50% solution)[62] and simulations (lines) with $k_{therm} = 0$ and (a) parameters given in Table 1 and conversion-dependent k_t given by eq 5 (-·-); (b) as in (a) except $k_{therm} = 4.8 \times 10^{-11}$ L mol^{-1} s^{-1} (– – –); (c) as in (a) except $k_d = 5.0 \times 10^6$ (···); (d) as in (a) except $[M]_0 = 4.3$ M, $[RX]_0 = [Mt^n]_0 = 0.045$ M (—).

linear fashion when plotted against $t^{1/3}$ once the initiation process is complete (after ~6 s$^{1/3}$ or ~200 s). The small amount of curvature at early times is due to the faster radical−radical termination rate of the initiating radical ($2k_{t0}$) relative to $2k_{tc}(0)$ and $2k_{td}(0)$.

There are some qualitative similarities between the kinetics predicted by the persistent radical effect and experiments, even though complete quantitative agreement is lacking. For example, the concentration of deactivating species that builds up is approximately the same, as is the rate of monomer consumption. Therefore, while some modifications to the model are required, the persistent radical effect appears to be underlying the kinetics of ATRP.

Inclusion of Diffusion-Controlled Termination. Figure 6 shows the first-order kinetic plot of styrene consumption in ATRP experiments (bulk and 50% solution) and several simulations. Each simulation includes a conversion-dependent termination rate according to eq 5 (or the appropriately modified version for the solution polymerization). The effects of thermal initiation of styrene and the rate of deactivation (k_d) on the rate of polymerization can also been seen. Including a conversion-dependent termination rate results in *straight* first-order kinetic plots. However, for the bulk polymerization, the apparent propagation rate (k_p^{app} = slope of the line) is too small compared with the experiment. A small decrease in k_d results in near perfect agreement. On the other hand, adding thermal initiation barely alters k_p^{app}. The conclusions that may be drawn from this is that (i) it is possible that k_d and/or k_a may contain some error or change during the reaction and (ii) k_p^{app} is not sensitive to thermal initiation in the ATRP of styrene under the conditions given here. For the solution polymerization, k_p^{app} is slightly overestimated. Adding thermal initiation to the solution polymerization has even less of an effect than observed for the bulk polymerization because of the lower monomer concentration.

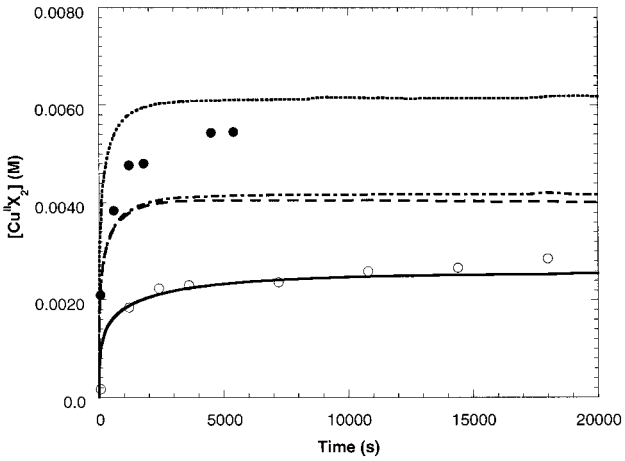

Figure 7. Dependence of $[Cu^{II}X_2]$ in the ATRP of styrene on conversion-dependent k_t, k_d, and k_{therm}. Experiment (●, bulk; ○, 50% solution)[64] and simulations (lines) with $k_{therm} = 0$ and (a) parameters given in Table 1 and conversion-dependent k_t given by eq 5 (-·-); (b) as in (a) except $k_{therm} = 4.8 \times 10^{-11}$ L mol^{-1} s^{-1} (– – –); (c) as in (a) except $k_d = 5.0 \times 10^6$ (···); (d) as in (a) except $[M]_0 = 4.3$ M, $[RX]_0 = [Mt^n]_0 = 0.045$ M (—).

Some comment should also be made in regard to the error associated with the activation and deactivation rate constants (k_a and k_d) used in our simulations. k_a was measured by a direct technique,[63] but under conditions that are not typical for a polymerization. k_d was then estimated from the equilibrium constant (K_{eq}) and the value of k_a ($k_d = k_a/K_{eq}$).[63] K_{eq} was measured under different conditions to k_a, with Mt^{n+1} (= $Cu^{II}X_2$) added at the beginning of the reaction so as to keep $[Cu^{II}X_2]$ constant.[62] However, subsequent EPR data showed that this is not the case, and $[Cu^{II}X_2]$ does increase slightly.[64] This would lead to an underestimation of K_{eq} and thus an overestimation of k_d. Therefore, the 50% difference observed in k_p^{app} between the simulations and the bulk experiment may, in part, be due to the error within the activation and deactivation rate constants. In addition, the simple first-order dependence of the rate of polymerization on $[Mt^n]$ and [RX], as was found experimentally for this system,[62] may not be always the case and is in fact not expected. We will discuss this further in a subsequent paper.[65]

Figure 7 shows that when a diffusion-dependent termination rate is included, the $[Mt^{n+1}]$ increases dramatically at the beginning of the polymerization and then levels out to be almost constant during the

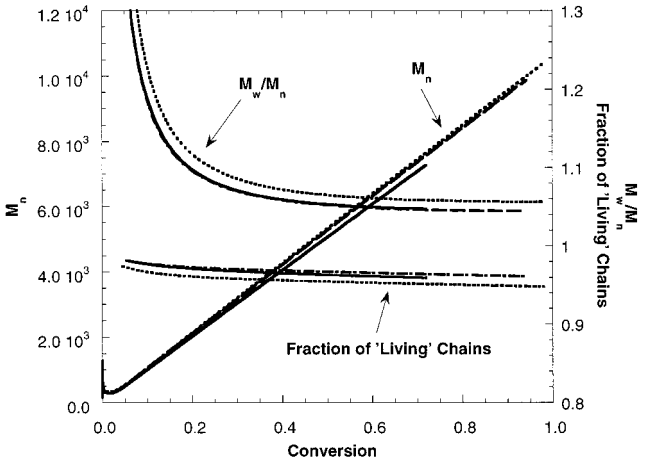

Figure 8. Number-average molecular weight (M_n), polydispersity (M_w/M_n), and fraction of "living" chains in the ATRP of styrene as a function of conversion. Simulations with $k_{therm} = 0$ and (a) parameters given in Table 1 and conversion-dependent k_t given by eq 5 (- · -); (b) as in (a) except $k_{therm} = 4.8 \times 10^{-11}$ L mol^{-1} s^{-1} (– – –); (c) as in (a) except $k_d = 5.0 \times 10^6$ (•••); (d) as in (a) except $[M]_0 = 4.3$ M, $[RX]_0 = [Mt^n]_0 = 0.045$ M (—).

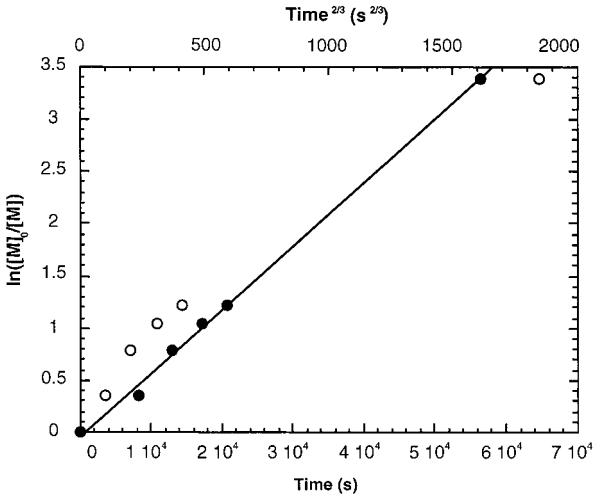

Figure 9. First-order kinetic plot of monomer consumption, as a function of time (○) and time$^{2/3}$ (●) (with linear fit, —), in the ATRP of MMA initiated by poly(methyl acrylate).[66] [PMA] = 0.0086 M ($M_n = 5910$, $M_w/M_n = 1.32$), $[MMA]_0 = 4.67$ M, $[CuCl]_0 = 0.017$ M, [4,4′-di(5-nonyl)-2,2′-bipyridyl]$_0 = 0.034$ M, 50% v/v diphenyl ether, 90 °C.

remainder of the reaction. In contrast, when a constant termination rate is used, the [Mt^{n+1}] continually increases. We have estimated the $Cu^{II}X_2$ (= Mt^{n+1}) concentration by EPR and found that approximately 5−6 mM of $Cu^{II}X_2$ is generated in bulk polymerizations and approximately 2−3 mM of $Cu^{II}X_2$ in solution polymerizations.[64] In bulk, the simulations where $k_d = 1.1 \times 10^7$ is used underestimate this concentration, whereas using $k_d = 5 \times 10^6$ the [Mt^{n+1}] is slightly overestimated. For the solution polymerization, the agreement between the simulation and experiment is excellent.

Another pathway that could lead to the apparent linear kinetics is the level of Mt^{n+1} present in the Mt^n catalyst. Further simulations, without diffusion-dependent termination, showed that adding approximately 2−5% Mt^{n+1} relative to Mt^1 was enough to produce a rate of polymerization approximately the same as that observed experimentally; however, some curvature in the first-order kinetic plot was still noticeable.

Figure 8 shows how the number-average molecular weight, polydispersity, and functionality of the polymer chains changes during the polymerization, using data from the same simulations from Figures 6 and 7. Clearly, in each case the molecular weight increases linearly and approaches the molecular weight predicted by the ratio of $([M]_0/[RX]_0) \times 104$ at full monomer conversion. The increase in M_n at very low conversions is actually to be expected and is due to chain growth when the concentration of the deactivator is very low. Hence, chains grow to be relatively long, but they also have a very low concentration. Once the deactivator concentration has built up (thus increasing the rate of deactivation), smaller chains are produced in higher concentrations, thus lowering M_n. This happens only at the very early stages of polymerization, and then the M_n will increase in the observed linear fashion. The polydispersity initially decreases rapidly and then is consistently around 1.05. Both of these phenomena are as observed in experiments.[62] Also evident is the high degree of chain functionality; throughout the polymerization greater than 95% of the chains contain a ω-terminal halide. This also agrees with experimental data.[63] The constancy of the functionality can be at least partly attributed to the reduction in the termination rate through the increase in viscosity. It is also noted that the slower deactivation step leads to a lower functionality, as would be expected.

Other Factors Affecting the Kinetics of ATRP. It is clear from the above discussion that the kinetics of ATRP are complex. We have shown that incorporating diffusion-dependent termination rate coefficients may effectively mask the persistent radical effect and that other rates may also be affected by an increase in viscosity. However, we were unable to obtain perfect agreement between the rates of polymerization, in both bulk and solution, and the simulations using the best rate data currently available.

As mentioned above, several factors may be contributing to this, such as poor experimental data (polymerization rates and rate constants), inhomogeneity, aggregation and/or deactivation of the Cu^I species by Cu^{II} species, poor choice of how rate coefficients varies with conversion, or the rate constants used either are incorrect or vary themselves throughout the reaction. It is quite possible that several of these phenomena may be operating concurrently. However, it is apparent from the simulations presented here that a qualitative picture of ATRP can be obtained. Further elucidation of both the mechanism and the rates of ATRP will no doubt improve the accuracy of our model.

Furthermore, the persistent radical effect may describe the kinetics of some ATRP systems quite well. We have noticed that, in polymerizations where a macroinitiator and/or solvents are used, the first-order kinetic plot may show curvature and indeed agree with the predicted $t^{2/3}$ dependence of eq 1. This is probably because k_t(DP) stays relatively constant in such reactions because viscosity changes are reduced. This means that, in contrast with low molar mass initiators, in the macroinitiator experiment the buildup of deactivator occurs relatively slowly and over the duration of the polymerization. Shown in Figure 9 is an example; here, the first-order kinetic plot for a poly(methyl acrylate)-initiated ATRP of methyl methacrylate (taken from ref 66) is plotted with $t^{2/3}$. The data fit very well to a straight line, and thus, in this system, the persistent

radical effect is not only operating but also quite observable.

Conclusions

It has been shown that controlled/"living" ATRP can be simulated using a model that incorporates a dynamic equilibrium between dormant and active (radical) chains (among other reactions). The persistent radical effect is present within the ATRP but may be somewhat concealed by the diffusion dependence of termination. The reduction in the termination rate during the polymerization also slows the production of the deactivating species, resulting in a steady rate of polymerization. Simulations that include this process have allowed reasonable reproduction of experimental data. It was also shown that thermal initiation of styrene does not contribute significantly to the rate of polymerization, or alter molecular weights or polydispersity, under the conditions examined. The evolution of molecular weights, polydispersity, and functionality with monomer conversion from the simulations agree well with experimental observations.

Experimental Section

The Predici program uses a discrete h−p method to represent chain length distributions and an adaptive Rothe method as a numerical strategy for time discretization. Concentrations of all species, as well as the distributions of all polymeric species, can be followed. The program has been applied and tested with various free radical polymerizations, including conventional,[29] pulsed laser,[30−32] and stable free radical[7] polymerizations. The conversion dependence of k_t(DP) was calculated using the interpreter function of Predici. For each time step, the degree of polymerization was calculated using DP = conversion × ($[M]_0/[RX]_0$). Using this DP, k_t(DP) was then calculated using eq 5 with the $k_t(0)$ value given in Table 1. For simulations of 50% solution ATRP experiments, the exponent in eq 5 was altered to −(0.65 + 0.01DP) to account for the lower polymer concentration. Using DP calculated in this way assumes that the two reacting radicals are of equal length, which for the most part is a reasonable assumption for ATRP where narrow distributions are obtained. It is only in the first ∼10% of the polymerization where this becomes less tenable (e.g., $M_w/M_n > 1.3$ at < 8% conversion in Figure 8). Calculations were performed on a personal computer (two 300 MHz processors) running Windows NT and took approximately 2−10 min to complete.

Acknowledgment. We thank the members of the ATRP Consortium at Carnegie Mellon University for financial support. D.A.S. further acknowledges support from Bayer Corp. through the Bayer Postdoctoral Fellowship at Carnegie Mellon University.

References and Notes

(1) Matyjaszewski, K., Ed. *Controlled Radical Polymerization*; ACS Symp. Ser. Vol. 685; American Chemical Society: Washington, DC, 1998.
(2) Solomon, D. H.; Rizzardo, E.; Cacioli, P. U.S. Pat. 4,581,429, 1986.
(3) Rizzardo, E. *Chem. Aust.* **1987**, *54*, 32.
(4) Fukuda, T.; Goto, A.; Ohno, K.; Tsujii, Y. In *Controlled Radical Polymerization*; Matyjaszewski, K., Ed.; ACS Symp. Ser. Vol. 685; American Chemical Society: Washington, DC, 1998; p 180.
(5) Georges, M. K.; Veregin, R. P. N.; Kazmaier, P. M.; Hamer, G. K. *Macromolecules* **1993**, *26*, 2987.
(6) Hawker, C. J. *Acc. Chem. Res.* **1997**, 3733.
(7) Greszta, D.; Matyjaszewski, K. *Macromolecules* **1996**, *29*, 7661.
(8) Zhu, Y.; Li, I. Q.; Howell, B. A.; Priddy, D. B. In *Controlled Radical Polymerization*; Matyjaszewski, K., Ed.; ACS Symp. Ser. Vol. 685; American Chemical Society: Washington, DC, 1998; p 214.
(9) Hammouch, S. O.; Catala, J. M. *Polym. Prepr. (Am. Chem. Soc., Div. Polym. Chem.)* **1997**, *38* (1), 655.
(10) Wang, J. S.; Matyjaszewski, K. *J. Am. Chem. Soc.* **1995**, *117*, 5614.
(11) Wang, J. S.; Matyjaszewski, K. *Macromolecules* **1995**, *28*, 7901.
(12) Kato, M.; Kamigaito, M.; Sawamoto, M.; Higashimura, T. *Macromolecules* **1995**, *28*, 1721.
(13) Percec, V.; Barboiu, B. *Macromolecules* **1995**, *28*, 7970.
(14) Granel, C.; Dubois, P.; Jerome, R.; Teyssie, P. *Macromolecules* **1996**, *29*, 8576.
(15) Haddleton, D. M.; Jasieczek, C. B.; Hannon, M. J.; Shooter, A. J. *Macromolecules* **1997**, *30*, 2190.
(16) Patten, T. E.; Xia, J.; Abernathy, T.; Matyjaszewski, K. *Science* **1996**, *272*, 866.
(17) Patten, T. E.; Matyjaszewski, K. *Adv. Mater.* **1998**, *10*, 901.
(18) Matyjaszewski, K.; Gaynor, S.; Wang, J. S. *Macromolecules* **1995**, *28*, 2093.
(19) Krstina, J.; Moad, G.; Rizzardo, E.; Winzor, C. L.; Berge, C. T.; Fryd, M. *Macromolecules* **1995**, *28*, 5381.
(20) Chiefari, J.; Chong, Y. K. B.; Ercole, F.; Krstina, J.; Jeffery, J.; Le, T. P. T.; Mayadunne, R. T. A.; Meijs, G. F.; Moad, C. L.; Moad, G.; Rizzardo, E.; Thang, S. H. *Macromolecules* **1998**, *31*, 5559.
(21) Matyjaszewski, K. In *Controlled Radical Polymerization*; Matyjaszewski, K., Ed.; ACS Symp. Ser. Vol. 685; American Chemical Society: Washington, DC, 1998; p 2.
(22) Gaynor, S. G.; Matyjaszewski, K. In *Controlled Radical Polymerization*; Matyjaszewski, K., Ed.; ACS Symp. Ser. Vol. 685; American Chemical Society: Washington, DC, 1998; p 396.
(23) (a) Fischer, H. *Macromolecules* **1997**, *30*, 5666. (b) Fischer, H. *J. Polym. Sci., Part A: Polym. Chem.*, submitted.
(24) Johnson, C. H. J.; Moad, G.; Solomon, D. H.; Spurling, T. H.; Vearing, D. J. *Aust. J. Chem.* **1990**, *43*, 1215.
(25) Daikh, B. E.; Finke, R. G. *J. Am. Chem. Soc.* **1992**, *114*, 2938.
(26) Fischer, H. *J. Am. Chem. Soc.* **1986**, *108*, 3925.
(27) Kothe, T.; Marque, S.; Martschke, R.; Popov, M.; Fischer, H. *J. Chem. Soc., Perkin Trans. 2* **1998**, 1553.
(28) Matyjaszewski, K. *J. Phys. Org. Chem.* **1995**, *8*, 197.
(29) Wulkow, M. *Macromol. Theory Simul.* **1996**, *5*, 393.
(30) Buback, M.; Busch, M.; Lämmel, R. A. *Macromol. Theory Simul.* **1996**, *5*, 845.
(31) Buback, M.; Lämmel, R. A. *Macromol. Theory Simul.* **1998**, *7*, 197.
(32) Hungenberg, K.-D.; Knoll, K.; Wulkow, M. *Macromol. Theory Simul.* **1997**, *6*, 393.
(33) Müller, A. H. E.; Yan, D.; Wulkow, M. *Macromolecules* **1997**, *30*, 7015.
(34) Matyjaszewski, K.; Davis, K.; Patten, T. E.; Wei, M. *Tetrahedron* **1997**, *53*, 15321.
(35) Hui, A. W.; Hamielec, A. E. *J. Appl. Polym. Sci.* **1972**, *16*, 749.
(36) Allen, P. E. M.; Patrick, C. R. *Makromol. Chem.* **1961**, *47*, 154.
(37) Benson, S. W.; North, A. M. *J. Am. Chem. Soc.* **1962**, *84*, 935.
(38) O'Driscoll, K. F. In *Comprehensive Polymer Science*; Eastmond, G. C., Ledwith, A., Russo, S., Sigwalt, P., Eds.; Comprehensive Polymer Science Vol. 3; Pergamon: London, 1989; p 161.
(39) Moad, G.; Rizzardo, E.; Solomon, D. H.; Beckwith, A. L. J. *Polym. Bull. (Berlin)* **1992**, *29*, 647.
(40) Heuts, J. P. A.; Gilbert, R. G.; Radom, L. *Macromolecules* **1995**, *28*, 8771.
(41) Griller, D. In *Landolt-Bornstein, New Series*; Fischer, H., Ed.; Springer-Verlag: Berlin, 1984; Vol. II/13a, p 5.
(42) Walbiner, M.; Wu, J. Q.; Fischer, H. *Helv. Chim. Acta* **1995**, *78*, 910.
(43) Fischer, H.; Paul, H. *Acc. Chem. Res.* **1987**, *20*, 200.
(44) Buback, M. *Makromol. Chem.* **1990**, *191*, 1575.
(45) Buback, M.; Kutcha, F.-D. *Macromol. Chem. Phys.* **1997**, *198*, 1455.
(46) Russell, G. T.; Napper, D. H.; Gilbert, R. G. *Macromolecules* **1988**, *21*, 2133.
(47) Russell, G. T.; Gilbert, R. G.; Napper, D. H. *Macromolecules* **1992**, *25*, 2459.
(48) Russell, G. T.; Gilbert, R. G.; Napper, D. H. *Macromolecules* **1993**, *26*, 3538.
(49) Russell, G. T. *Macromol. Theory Simul.* **1994**, *3*, 439.

(50) Russell, G. T. *Macromol. Theory Simul.* **1995**, *4*, 497.
(51) de Kock, J. B. L.; Klumpermann, B.; van Herk, A. M.; German, A. L. *Macromolecules* **1997**, *30*, 6743.
(52) Moad, G.; Shipp, D. A.; Smith, T. A.; Solomon, D. H. *Macromolecules* **1997**, *30*, 7627.
(53) Yasukawa, T.; Takahashi, T.; Murakami, K. *J. Chem. Phys.* **1972**, *57*, 2591.
(54) Yasukawa, T.; Murakami, K. *Polymer* **1980**, *21*, 1423.
(55) Olaj, O. F.; Zifferer, G. *Makromol. Chem., Rapid Commun.* **1982**, *3*, 549.
(56) Olaj, O. F.; Vana, P. *Macromol. Rapid Commun.* **1998**, *19*, 433.
(57) Olaj, O. F.; Vana, P. *Macromol. Rapid Commun.* **1998**, *19*, 533.
(58) Karatekin, E.; O'Shaughnessy, B.; Turro, N. J. *Macromolecules* **1998**, *31*, 4655.
(59) Griffiths, M. C.; Strauch, J.; Monteiro, M. J.; Gilbert, R. G. *Macromolecules* **1998**, *7835*, 5.
(60) Piton, M. C.; Gilbert, R. G.; Chapman, B. E.; Kuchel, P. W. *Macromolecules* **1993**, *26*, 4472.
(61) Moad, G.; Solomon, D. H. *The Chemistry of Free-Radical Polymerization*; Pergamon: Oxford, 1995.
(62) Matyjaszewski, K.; Patten, T. E.; Xia, J. *J. Am. Chem. Soc.* **1997**, *119*, 674.
(63) Ohno, K.; Goto, A.; Fukuda, T.; Xia, J.; Matyjaszewski, K. *Macromolecules* **1998**, *31*, 2699.
(64) Kajiwara, A.; Matyjaszewski, K.; Kamachi, M. *Macromolecules* **1998**, *31*, 5695.
(65) Shipp, D. A.; Matyjaszewski, K., manuscript in preparation.
(66) Shipp, D. A.; Wang, J.-L.; Matyjaszewski, K. *Macromolecules* **1998**, *31*, 8005.
(67) Buback, M.; Gilbert, R. G.; Hutchinson, R. A.; Klumperman, B.; Kuchta, F.-D.; Manders, B. G.; O'Driscoll, K. F.; Russell, G. T.; Schweer, J. *Macromol. Chem. Phys.* **1995**, *196*, 3267.
(68) Berger, K. C.; Meyerhoff, G. In *Polymer Handbook*; Brandup, J., Immergut, E. H., Eds.; Wiley: New York, 1989; p II/67.

MA9819135